

Article

The Layered Encapsulation of Vitamin B₂ and β-Carotene in Multilayer Alginate/Chitosan Gel Microspheres: Improving the Bioaccessibility of Vitamin B₂ and β-Carotene

Peilong Liao ¹ , Shicheng Dai ¹, Ziteng Lian ¹, Xiaohong Tong ¹, Sai Yang ¹, Yashuang Chen ¹, Weijie Qi ¹, Xinhui Peng ¹, Huan Wang ^{1,2,*} and Lianzhou Jiang ^{1,3}

- ¹ College of Food Science, Northeast Agricultural University, Harbin 150030, China; liaopeilong@neau.edu.cn (P.L.); 18443602143@163.com (S.D.); lianziteng@neau.edu.cn (Z.L.); tongxiaohong0110@163.com (X.T.); S201001027@neau.edu.cn (S.Y.); cys18337336195@163.com (Y.C.); 15725237855@189.cn (W.Q.); s201001904@neau.edu.cn (X.P.); jlzname@neau.edu.cn (L.J.)
- ² Key Laboratory of Soybean Biology of Chinese Education Ministry, Harbin 150030, China
- ³ School of Tea and Food Science & Technology, Anhui Agricultural University, Hefei 230036, China
- * Correspondence: whname@neau.edu.cn; Fax: +86-0451-55190477



Citation: Liao, P.; Dai, S.; Lian, Z.; Tong, X.; Yang, S.; Chen, Y.; Qi, W.; Peng, X.; Wang, H.; Jiang, L. The Layered Encapsulation of Vitamin B₂ and β-Carotene in Multilayer Alginate/Chitosan Gel Microspheres: Improving the Bioaccessibility of Vitamin B₂ and β-Carotene. *Foods* **2022**, *11*, 20. <https://doi.org/10.3390/foods11010020>

Academic Editors: Yaqiong Zhang and Xin Jia

Received: 22 November 2021

Accepted: 17 December 2021

Published: 22 December 2021

Publisher's Note: MDPI stays neutral with regard to jurisdictional claims in published maps and institutional affiliations.



Copyright: © 2021 by the authors. Licensee MDPI, Basel, Switzerland. This article is an open access article distributed under the terms and conditions of the Creative Commons Attribution (CC BY) license (<https://creativecommons.org/licenses/by/4.0/>).

Abstract: This research underlines the potential of alginate multilayered gel microspheres for the layered encapsulation and the simultaneous delivery of vitamin B₂ (VB) and β-carotene (BC). Chitosan was used to improve the stability and controlled release ability of alginate-based gel microspheres. It was shown that a clear multilayered structure possessed the characteristics of pH response, and excellent thermal stability. The sodium alginate concentration and the number of layers had notable effects on mechanical properties and particle size of gel microspheres. Fourier-transform infrared spectroscopy and X-ray diffraction analyses further proved that VB and BC were encapsulated within the gel microspheres. Compared with the three-layer VB-loaded gel microspheres, the total release of VB from the three-layer VB and BC-loaded gel decreased from 93.23% to 85.58%. The total release of BC from the three-layer VB and BC-loaded gel increased from 66.11% to 69.24% compared with three-layer BC-loaded gel. The simultaneous encapsulation of VB and BC in multilayered gel microspheres can markedly improve their bioaccessibility and bioavailability. These results showed the multilayer gel microspheres synthesized herein have potential for applications in the layered encapsulation and simultaneous delivery of various bioactive substances to the intestinal tract.

Keywords: pH response; core-shell structure; simultaneous delivery; bioaccessibility

1. Introduction

In recent years, several structured biopolymer-based matrices and carriers have already been developed to encapsulate and protect water-soluble or lipid-soluble bioactive substances [1–4]. Currently, various established delivery systems such as nanoparticles, microcapsules, multi-layer emulsion, and polymer-drug conjugates, are being used for the delivery of multiple bioactive substances [5–8].

Vitamins play an important role in the regulation of body functions. Vitamin B₂ (VB), also known as riboflavin, is a water-soluble vitamin. β-carotene (BC), as an important member of the carotenoid family, which is a precursor substance of vitamin A. Both VB and BC are mainly absorbed in the colon, these substances have the ability to scavenge free radicals, improve vision, boost immunity, and protect skin health [9]. Indeed, Vitamins and carotenoids usually display a synergistic effects and have shown improvements in their functional properties for the human body when they were prescribed together [10,11]. A previous research showed that sufficient intake of both BC and VB could help prevent cognitive decline among elderly men with diabetes mellitus [12]. While VB is stable in acidic conditions, and it is destroyed under alkaline conditions, the opposite is true for BC [13]. Furthermore, the low solubility and bioavailability of VB and BC, limit their efficient transit

and absorption in the human body [13]. Thus, there may be a major challenge associated with the development of delivery systems that can simultaneously encapsulate and deliver vitamin B₂ and β -carotene on the same carriers.

The construction of gel-based delivery and a controlled release system had attracted much attention, as it simultaneously delivered various bioactive substances. Sodium alginate (SA) is an acidic polysaccharide rich in anions [14]. It has excellent biocompatibility, non-toxicity, and immunogenicity, owing to which it has been widely used for the delivery of bioactive substances [15–18]. However, there are still some limitations associated with the use of an alginate-gel based delivery system: alginate-based gel microspheres are highly porous and show a weak network, low adherence, and high burst release properties [19]. Fortunately, blending SA with other polymers is an effective method to circumvent these problems. Chitosan (CS), a type of cationic polysaccharide rich in amines, has been widely used in various pharmaceutical applications [20,21]. Previous research investigations have shown that chitosan not only improves the overall stability of the alginate beads, but also notably delays their release via the formation of electrostatic interactions [22–24]. Bajpai et al. [17] prepared calcium alginate/chitosan multilayered beads for delayed release of vitamin B₂. Belščak et al. [25] used a latex/internal gel method to prepare gel microspheres that could simultaneously transport hydrophilic (from dandelion extract) polyphenols and β -carotene. Yadav et al. [26] reported that chitosan can fortify calcium alginate microspheres for the controlled delivery of dual drugs.

It has been speculated that the multilayered gel microspheres have the potential for layered encapsulation and protection for vitamin B₂ and β -carotene from the external environment. To the best of our knowledge, thus far, no reports have investigated the simultaneous release behavior and bioavailability of VB and BC when they were layered encapsulated within multilayered gel microspheres. In this study, BC and VB were utilized as the model drugs and soybean protein isolate (SPI) was used as the aqueous phase. VB and BC were encapsulated within gel microspheres, which formed VB-in-gel layer-BC-in-gel layer systems. The swelling characteristics, particle size and mechanical properties, microstructure, and thermal stability of the prepared multilayered gel microspheres were evaluated. In addition, Fourier transform infrared spectroscopy (FT-IR) and X-ray diffraction (XRD) were used to analyze the interaction between SA and CS, and the encapsulation of VB and BC. The release behavior of VB and BC and the effects of multilayered structures on their bioavailability and bioaccessibility were further investigated via *in vitro* analyses of their release from the multilayer gel microspheres.

2. Materials and Methods

2.1. Materials

Chitosan (CS, level of deacetylation, 97%; $\geq 99.5\%$ purity), Sodium alginate (SA, molecular weight in the range of 90–150 kDa; $\geq 97.7\%$ purity), Calcium chloride ($\geq 96.0\%$ purity), β -carotene, BC ($\geq 98\%$ purity) and Vitamin B₂, VB ($\geq 97\%$ purity) were bought from Yuanye Biotechnology Co., Ltd. (Shanghai, China). Soybean protein isolate (SPI, 91.6% protein) was purchased from DuPont Shineway Food Co., Ltd. (Luohe, China). The other chemicals were purchased from local shops in China.

2.2. Preparation of Sample

2.2.1. Preparation of Chitosan-Alginate Core-Shell Gel Microspheres (L₁)

The sodium alginate (SA) solution with varying concentrations (0.5%, 1%, 1.5%, 2.0%, and 2.5% *w/v*) were prepared by dispersing SA into distilled water; the pH value was adjusted to 5.0 using 1.0 M sodium hydroxide solution and hydrochloric acid solution. Then, CS powder was pre-dissolved in 1% acetic acid aqueous solution. The gelation medium consisted of 0.6% (*w/v*) CS and 5% (*w/v*) CaCl₂, followed by adjusting the pH to 5.0. The SA solution was dropped into the gelation medium at room temperature with constant stirring and the flow rate was controlled at approximately 15 drops/min. The gel microspheres were allowed to stand in the gelation medium for 10 min and then removed.

The microspheres were then washed with distilled water and dried at 35 °C until they reached constant weight. These gel microspheres shall henceforth be denoted as sample L₁.

2.2.2. Preparation of Multilayered Gel Microspheres (L_n)

To prepare multilayered gel microspheres, the process of the sample L₁ was repeated and the two-layer gel microspheres obtained. There were immediately put L₁ into the SA solution for 20 min and then transferred into the gelation medium for 10 min. Then the gel microspheres were taken out and washed with distilled water, dried at 35 °C. These gel microspheres were named as sample L₂. The three-layer gel microspheres were prepared by repeating the process above. These gel microspheres shall be denoted as sample L₃.

2.2.3. Preparation of VB-Loaded Gel Microspheres (L-VB)

The VB-loaded gel microspheres (containing VB in the core) were obtained by dropping the SA solution (pH 5.0) with vitamin B₂ (0.25%, *w/v*) into the gelation medium. The one-layer VB-loaded gel microspheres shall be denoted as sample L₁-VB. Then these microspheres were mixed repeatedly with the same SA solution to form multilayered gel microspheres. The two-layer and three-layer VB-loaded gel microspheres shall be denoted as sample L₂-VB and L₃-VB, respectively.

2.2.4. Preparation of BC-Loaded Gel Microspheres (L-BC)

First, β-carotene was suspended in corn oil (0.5%, *w/v*). Then, an aqueous solution of 2.5% (*w/w*) (of proteins) SPI and corn oil (containing BC was emulsified (ULTRA-TURRAX, T18, IKA, Staufen, Germany) at 10,000 rpm/min for 3 min and homogenized at 60 MPa for three times to form an emulsion; next, the solution of SA was mixed with the emulsion at a ratio of 1:1 to form an emulsion-filled sol. The BC-loaded gel microspheres (containing BC in the core) were obtained by adding the emulsion-filled sol with BC (0.25%, *w/v*) into the gelation medium in a dropwise manner. The one-layer BC-loaded gel microspheres shall be denoted as sample L₁-BC. Then these gel microspheres were mixed repeatedly with the SA solution to form multilayered gel microspheres. The two-layer and three-layer BC-loaded gel microspheres shall be denoted as sample L₂-BC and L₃-BC, respectively.

2.2.5. Preparation of VB-BC-Loaded Gel Microspheres (L-VB-BC)

To prepare VB-BC-loaded gel microspheres (L₃-VB-BC), the L₁-VB gel microspheres were mixed with the emulsion-filled sol to form two-layer gel microspheres (L₂-VB-BC), which were then transferred into the gelation medium for 10 min. These gel microspheres were mixed with the SA solution to form the three-layer gel microspheres gel microspheres (L₃-VB-BC).

2.3. Swelling Study of Gel Microspheres

Briefly, the swelling property of the gel microspheres was measured according to the methods described by Sun et al. [27]. The pre-weighed gel microspheres were immersed in 0.1 M phosphate buffered solution (PBS) with pHs 2.0, and 7.4 at 37 °C, which served as the simulating fluid. The PBS was composed of disodium hydrogen phosphate and sodium dihydrogen phosphate and the pH was adjusted using 0.1 M HCl. At every 1-h interval, the swollen gel microspheres were weighed immediately after removing the excess droplets attached onto the surface of the gel microspheres using a filter paper. The weight change was measured for 6 h. The weight change was converted to a percentage using the formula shown below (1):

$$\text{Dynamic weight change} = \frac{\text{Final weight} - \text{Initial weight}}{\text{Initial weight}} \times 100\% \quad (1)$$

The measurements were repeated five times for all samples and the calculations were performed using the average data.

2.4. The Mechanical Properties of the Gel Microspheres

The fracture values (hardness and springiness) of the gel microspheres were measured using a TAXT plus analyzer apparatus (Stable Micro Systems, Godalming, UK) according to the method of Feng et al. [18]. The tests were performed on twenty gel microspheres using a P 35 cylindrical measurement probe. The trigger force and squeezing depth of the samples were set at 5 g and 10 mm at a rate of 1.0 mm/s, respectively. The compression of the gel microspheres was 40%. Each test was repeated three times. The hardness and springiness data were collected for range analysis and the optimal group of samples was selected.

2.5. Particle Size Measurement

The particle size of the gel microspheres was estimated as described by Ma et al. [28] with minor modifications. The particle size of the gel microspheres was measured previously using a digital caliper (0–150 mm, DL91150, Precisional Measuring Tool, Deli Instruments, Ningbo, China). Thirty dried gel microspheres were selected and their particle size was measured with an accuracy of ± 0.01 mm.

2.6. Differential Scanning Calorimetry (DSC) Analysis

The thermal stability of the gel microspheres was measured by using the method described by Fareez et al. [29]. About 10.0 mg of powders of gel microspheres (L_1 , L_2 , and L_3) were placed in a ceramic crucible and DSC curves were constructed using a DSC instrument (DSC 3, Mettler Toledo, Greifensee, Switzerland). The analysis was performed at a temperature range of 20–200 °C at 10 °C/min and a dry flow of N_2 .

2.7. Analysis of the Microstructure of the Gel Microspheres

2.7.1. Optical Microscopy (OM)

The morphology of the gel microspheres was observed using an optical microscope (BX53, Olympus Co. Ltd., Beijing China). Before observation, a thin layer of each gel microsphere (approximately 1 mm) was cut and placed on a glass slide.

2.7.2. Confocal Laser Scanning Microscopy (CLSM)

Following the method of Lin et al. [30], each gel microsphere was cut into a thin layer (approximately 1 mm) and stained for 30 min. The staining solution was prepared by mixing Nile red (0.1%, w/v , in isopropyl alcohol) and Nile blue (0.1%, w/v , in isopropyl alcohol) at a ratio of 1:1. Confocal microscopy images were obtained using a Leica SP8 microscope (Leica Microsystems GmbH, Wetzlar, Germany), using excitation and emission wavelengths of 488 and 515 nm, respectively.

2.7.3. Scanning Electron Microscopy (SEM)

The morphology of the gel microspheres (PP3010T, Hitachi High-Technologies Corp., Tokyo, Japan) was obtained following the method described by Qin et al. [20], with slight modifications. Before observation, the gel microspheres were frozen, then the gel microspheres were sputter-coated with gold.

2.8. FT-IR Spectroscopy

The SA, CS, VB, BC, L_3 , 1.5% SA L_3 -VB-BC and 2.5% SA L_3 -VB-BC samples were studied using a Fourier transform infrared spectrophotometer (FT-IR; Thermo Fisher Technology Co., LTD, Shanghai, China). The FT-IR spectra were recorded on an FT-IR spectrophotometer, ranging from 4000 to 400 cm^{-1} , using KBr pellets.

2.9. X-ray Diffraction (XRD) Analysis

The test conditions used for XRD analysis (Malvern Paralytical, Almelo, The Netherlands) were as follow: 2θ ranging from 5° to 70°; Cu was utilized as the light source. The generator voltage and tube current were set to 45 kV and 40 mA, respectively.

2.10. Release Studies

2.10.1. Drug Loading Capacity (LC) Measurement

To determine the drug loading capacity of the gel microspheres, a certain mass of the VB or BC-loaded gel microspheres (0.50 g) was dried and ground to a fine powder. The powder was then placed in PBS (50 mL; pH 7.4) and shaken for 24 h at 30 °C in a water bath. After the drug was completely extracted from all the test gel microspheres, filtration was performed and the filtrate was reserved for later use.

The content of VB was measured by Bajpai and Tankhiwale's [17] reported approach. Five milliliter aliquots of the filtrate were centrifuged at $2000 \times g$ for 5 min. The clear liquid in the middle layer was collected and then measured at 255 nm.

According to the methods described in Donhowe et al. and Roman et al. [31,32] reported to measure the content of BC, 5-mL aliquots of the filtrate were extracted with 5 mL of acetone: ethanol: hexane (25 mL:25 mL:50 mL, respectively), inverted 10 times and placed in capped test tubes. The top layer was collected and additional extractions were performed with 1 mL of n-hexane. After extraction, the content of BC was measured at 450 nm. The drug loading capacity was calculated as follows (2):

$$LC \text{ (mg/g)} = \frac{\text{Total bioactive(vitamin B}_2 \text{ or } \beta \text{ - carotene)}}{\text{Weight of bioactive - loaded gel microspheres}} \quad (2)$$

2.10.2. Drug Release Experiments

The release of the substances from the gel microspheres was analyzed according to the method described by Umaredkar et al. [33], with some modifications. The L₁-VB, L₃-VB, L₁-BC, L₃-BC and L₃-VB-BC samples were performed in PBS (pH 2.0) for the first 2 h, then transferred to PBS with a pH 7.4 from 3 to 10 h. The bath parameters were set using an orbital shaking water bath as follows: 120 rpm/min, maintained at 37 ± 0.5 °C (SHA-B, Mycono Instruments Co., Ltd., Changzhou, China). At 1-h intervals, 5 mL aliquots were drawn and filtered every 1-h intervals using a pipette gun during a 10 h period. The 5 mL of an equivalent fresh dissolution medium was added to maintain the same conditions after withdrawing each sample.

According to the method described in Section 2.10.1, the extent of release of VB or BC during digestion was evaluated as follows (3):

$$\text{Release (\%)} = \frac{\text{Released bioactive(vitamin B}_2 \text{ or } \beta \text{ - carotene)}}{\text{Total bioactive(vitamin B}_2 \text{ or } \beta \text{ - carotene)}} \quad (3)$$

2.10.3. Bioaccessibility, Stability, and Bioavailability of VB and BC

The bioaccessibility, stability, and bioavailability of VB or BC were determined after simulated small intestinal digestion [34]. After in vitro simulated digestion, according to the method described in Section 2.10.1, the concentration of VB or BC was measured. The bioaccessibility, stability, and bioavailability of VB or BC were calculated as follows (4), (5) and (6), respectively, as shown below:

$$\text{Bioaccessibility} = \frac{C_M}{C_D} \times 100\% \quad (4)$$

$$\text{Stability} = \frac{C_D}{C_I} \times 100\% \quad (5)$$

$$\text{Bioavailability} = \frac{C_M}{C_I} \times 100\% \quad (6)$$

In these formulae C_I , C_M , and C_D are the concentrations of VB or BC added initially, in the micelle fraction and in the total digesta at the end of the small intestinal digestion, respectively.

2.11. Statistical Analysis

All experiments were performed within 12 h of the preparation of samples prepared. Each test was performed at least twice in independent assays. Data analysis was performed using Origin 2019 (Origin Lab, Northampton, MA, USA). The results were analyzed by one-way analysis of variance (ANOVA) and Duncan's multiple range test using the Statistica 20 software.

3. Results and Discussion

3.1. FT-IR Spectroscopy and XRD Analysis

FT-IR spectroscopy is used to analyze the structural changes of substances. The FT-IR spectra of SA are shown in Figure 1A. The stretching vibrations of the O–H and C–H bonds are assigned at 3423.58 cm^{-1} and 2925.67 cm^{-1} , respectively [35]. The peaks near 1437.23 cm^{-1} were caused by symmetric and asymmetric stretching vibrations of COO– groups. In Figure 1A CS, the peak at 3423.42 cm^{-1} is attributed to the O–H stretching vibrations. The bending vibration of N–H and the stretching vibration of C=O are observed at 1597.68 cm^{-1} and 1654.42 cm^{-1} , respectively [35,36]. The peaks at 1258.15 cm^{-1} and 1064.33 cm^{-1} represent C–O stretching vibrations, which are common structures in CS.

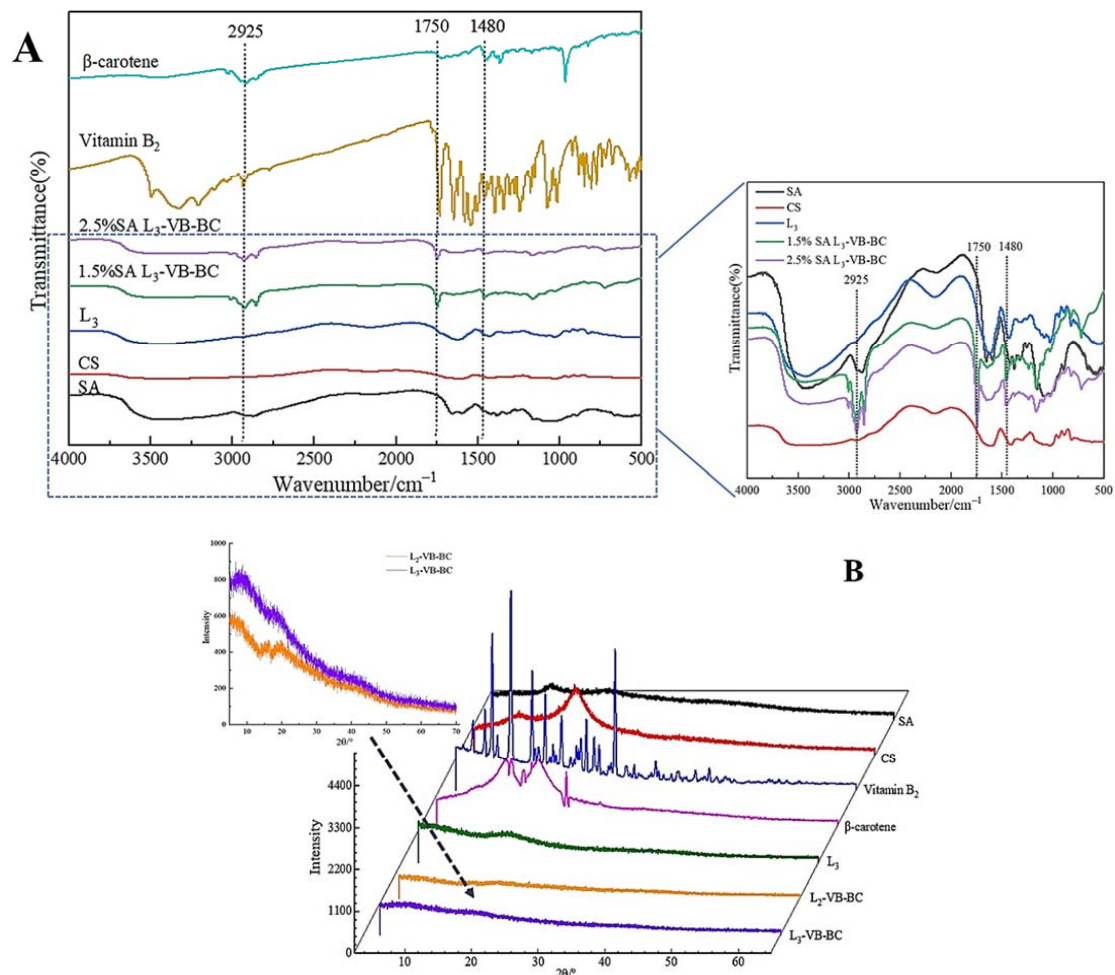


Figure 1. FT-IR and XRD of SA, CS, vitamin B₂ (VB), β -carotene (BC) and gel microspheres. (A) FT-IR analysis of SA, CS, the three-layer-gel microspheres (L₃), 1.5% SA VB and BC-loaded gel microspheres (1.5% SA L₃-VB-BC), 2.5% SA VB and BC-loaded gel microspheres (2.5% SA L₃-VB-BC), VB, and BC; (B) X-ray diffraction images of SA, CS, VB, BC, the three-layer-gel microspheres (L₃), two-layer VB and BC-loaded gel microspheres (L₂-VB-BC), and three-layer VB and BC-loaded gel microspheres (L₃-VB-BC).

The FT-IR spectroscopy of multilayered gel microspheres L_3 differed markedly from the aforementioned observations, as shown in Figure 1. The peaks at 1597.68 cm^{-1} and 3423.42 cm^{-1} were shifted to 1617.45 cm^{-1} and 3470.21 cm^{-1} , respectively, in case of the L_3 microspheres. The asymmetric stretching vibrations of COO^- groups changed from 1420.57 cm^{-1} to 1437.24 cm^{-1} , which can be attributed to the cross-linking of Ca^{2+} ions with SA [37]; these changes indicated the cross-linking of Ca^{2+} ions and the polyelectrolyte complexation reaction of CS with SA [26]. The absorption peaks at 2925.57 cm^{-1} and 2854.43 cm^{-1} were caused by the vibration of the hydrophobic group CH_2 in BC (Figure 1A β -carotene). 1746.41 cm^{-1} and 3009.11 cm^{-1} represent C–O stretching vibrations, which were common structures in VB (Figure 1A Vitamin B_2). There were no significant changes in these peaks (Figure 1A L_3 -VB-BC), indicating that vitamin B_2 and β -carotene were encapsulated within the gel microspheres.

In order to further prove that the vitamin B_2 and β -carotene were encapsulated in the multilayer gel microspheres, CS, SA, the three-layer-gel microspheres (L_3), VB, BC, VB and BC-loaded gel microspheres (L-VB-BC) were analyzed by XRD. For VB (Figure 1B), numbers of crystalline peaks were seen in the region of 10° – 30° , suggesting VB had a clear crystal structure. The XRD pattern of BC (Figure 1B) shows there are strong peaks between 13° and 25° , indicating that BC has a highly crystalline structure [38]. While SA shows a typical smooth curve, the XRD patterns of CS did not accord with the result described by Ji et al. [24], in which CS showed strong peaks at 19.94° (Figure 1B CS), indicating the presence of different crystal morphologies. The three-layer-gel microspheres (L_3) had a weak diffraction peak at 18.27° , suggesting it was significantly influenced by CS [39]. Compared to VB and BC, most of these peaks disappeared in the VB and BC-loaded gel microspheres, which was associated with low concentration of VB and BC. These changes were attributed to the increase in the proportions of molecules with higher degrees of freedom in the crystal structure, which can obscure the crystallinity of VB and BC [29]. The outcomes of XRD further confirm the dispersion of drugs into the gel microspheres.

3.2. CLSM of Gel Microspheres

The encapsulation of BC by the multilayered gel microspheres was investigated by CLSM analysis. The oil and protein were stained with Nile red and Nile blue, respectively (Figure 2). The gel microspheres show a notable core-shell structure, which is consistent with the structure observed in the microscopy analysis. Figure 2A shows that the proteins and oils are distributed in the shell layer. Interestingly, as shown in Figure 2B, both oils and proteins are distributed within the inside of the gel microspheres. These results indicate that bioactive substances can be layered encapsulated within multilayered gel microspheres. The multilayered structure confers the property of simultaneously carrying a variety of bioactive substances.

3.3. Mechanical Properties and Particle Size of the Gel Microspheres

It is known that the degree of deformation of gel microspheres under the action of applied external force is related to the particle size, number of layers, SA concentration and shell thickness [40], as shown in Table 1. The hardness and springiness of the gel microspheres increased with the concentration of SA and the increase in the number of layers, mainly due to the increase in the degree of cross-linking between Ca^{2+} and SA [41], which reflected that the higher the SA concentration, the denser is the shell structure. Thus, it may be inferred that the design of gel microspheres with different mechanical properties and physical properties can be achieved by varying the number of layers.

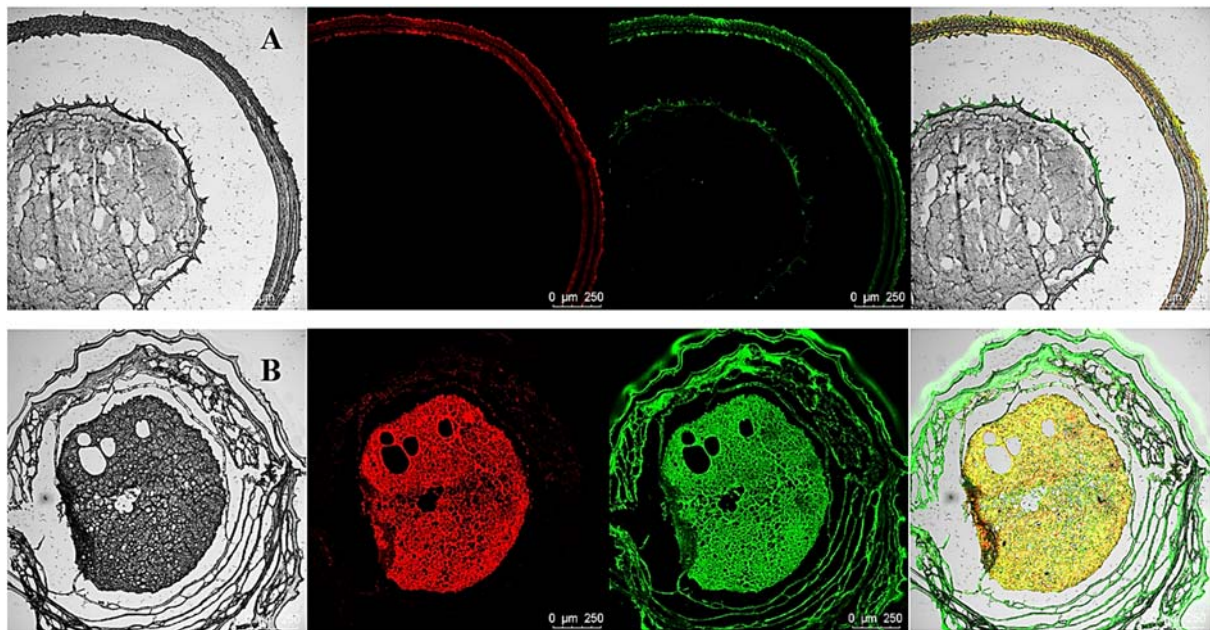


Figure 2. Confocal microscopy images of three-layer BC-loaded-gel microspheres (L_3 -BC) with embedding at different locations. Confocal microscopy images of 2.5% SA three-layer BC-loaded-gel microspheres (A). Confocal microscopy images of 1.5% SA three-layer BC-loaded-gel microspheres (B). The images were obtained by conventional optical microscopy and confocal fluorescence microscopy after sectioning the samples using a microtome.

Table 1. Springiness and hardness of gel microspheres.

Sample	L_1		L_2		L_3	
	Hardness(g)	Springiness	Hardness(g)	Springiness	Hardness(g)	Springiness
0.5% SA	54.04 ± 0.49 ^e	0.607 ± 0.005 ^d	68.81 ± 0.25 ^e	0.749 ± 0.012 ^d	183.62 ± 0.58 ^e	0.79 ± 0.004 ^d
1.0% SA	59.90 ± 0.44 ^d	0.712 ± 0.006 ^c	74.34 ± 0.92 ^d	0.772 ± 0.004 ^c	368.56 ± 1.88 ^d	0.866 ± 0.0042 ^c
1.5% SA	65.15 ± 0.22 ^c	0.787 ± 0.006 ^b	112.13 ± 0.27 ^c	0.796 ± 0.007 ^b	457.14 ± 1.20 ^c	0.923 ± 0.006 ^b
2.0% SA	86.76 ± 0.34 ^b	0.833 ± 0.03 ^a	164.73 ± 0.71 ^b	0.885 ± 0.003 ^a	589.96 ± 1.67 ^b	0.968 ± 0.004 ^a
2.5% SA	135.61 ± 0.46 ^a	0.852 ± 0.13 ^a	442.75 ± 1.07 ^a	0.891 ± 0.052 ^a	632.12 ± 0.04 ^a	0.959 ± 0.008 ^a

L_1 : the one-layer-gel microspheres; L_2 : the two-layer-gel microspheres; L_3 : the three-layer-gel microspheres. Values with different superscript letters are significantly different ($p < 0.05$).

The variation of the particle size of gel microspheres is shown in Figure 3. When the concentration of SA increased from 0.5% to 1.5%, the particle size of the one-layer gel microspheres (L_1) increased significantly from 1.50 to 2.25 mm ($p < 0.05$). This was attributed to the fact that the shape of the gel microspheres formed was associated with the deformation of the droplet as it impacted the motionless gelation bath surface [37]. When the SA concentration was higher than 1.5%, this effect can be ignored, thus, the particle size tended to stabilize. The particle size of the multilayered gel microspheres increased markedly with an increase in the number of layers, which was consistent with the findings of a study by Anal et al. [42]. The maximum diameter of three-layer gel microspheres (L_3) was 4.21 mm, while the minimum diameter was 2.23 mm. Higher the SA concentrations allowed for higher surface tension and thicker crusts, indicating that more SA remained on the multilayer gel microspheres as the SA concentration increased [43]. This further indicated the formation of a multi-layered structure.

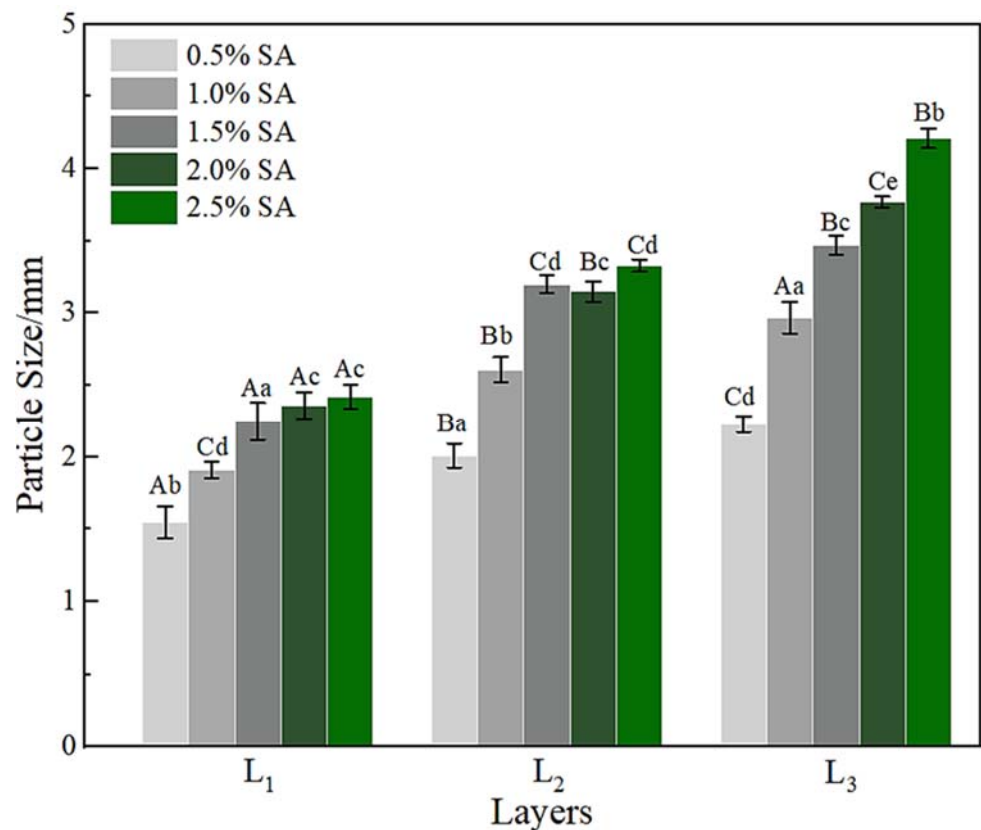


Figure 3. The particle size of L₁, L₂, and L₃. L₁: the one-layer-gel microspheres; L₂: the two-layer-gel microspheres; L₃: the three-layer-gel microspheres. Different lowercase letters indicate significant differences ($p < 0.05$) of the particle size within the same number of layers. Different capital letters indicate significant differences ($p < 0.05$) of the particle size between different number of layers.

3.4. DSC Analysis of the Gel Microspheres Measurement

DSC can characterize the behavior of mixed phases in polymer blend systems, thus, demonstration of the thermal stability of the polymers can be ascertained (Figure 4) [44]. The DSC thermogram of the multilayered gel microspheres (L₁, L₂, and L₃) showed that all the endothermic peaks occurred at more than 100 °C. It can also be anticipated that the other samples should also show excellent thermally stability below 100 °C. This reduction in the melting temperature of gel microspheres increased with an increase in the number of layers. This was related to the evaporation of water (both surface and crystallization water) in the gel microspheres [45,46], where more water molecules were evaporated with an increase in the number of layers. This study was focused on developing gel microspheres that can be used for oral drug delivery; it can demonstrate that the gel microspheres exhibit favorable stability of the body temperature (i.e., 37 °C).

3.5. Microstructure of Gel Microspheres

The internal microstructure of the gel microspheres was observed using a microscope; these results are shown in Figure 5. The microspheres usually exhibit a spherical shell-like architecture with multiple layers inside each microsphere (Figure 5A,B). Therefore, the internal structure of the gel microspheres was further observed by scanning electron microscopy (SEM). The SEM image of multilayered gel microspheres (Figure 5C) shows that there are voids between the layers that can be used to preserve the drug, as described by Li et al. [43]. The optical microscopic image (Figure 5D) further shows that the gel microspheres had an obvious multi-layer structure. The multi-layer structure of the gel microspheres became denser and smoother as the concentration of SA increased. These findings may be related to the polycation properties of CS, which competed with Ca²⁺

to interact with the polyelectrolytes of SA [37]. When the concentration of SA increased, this competitive effect gradually diminished, leading to the formation of a denser shell. Lim et al. [47] reported that there was a loose gel structure of the gel microspheres, which showed weak gelation due to low concentrations of SA. Moreover, there were traces of tearing inside the gel microspheres; this may be because the internal structure of the gel microspheres was damaged to a certain extent during the sectioning process.

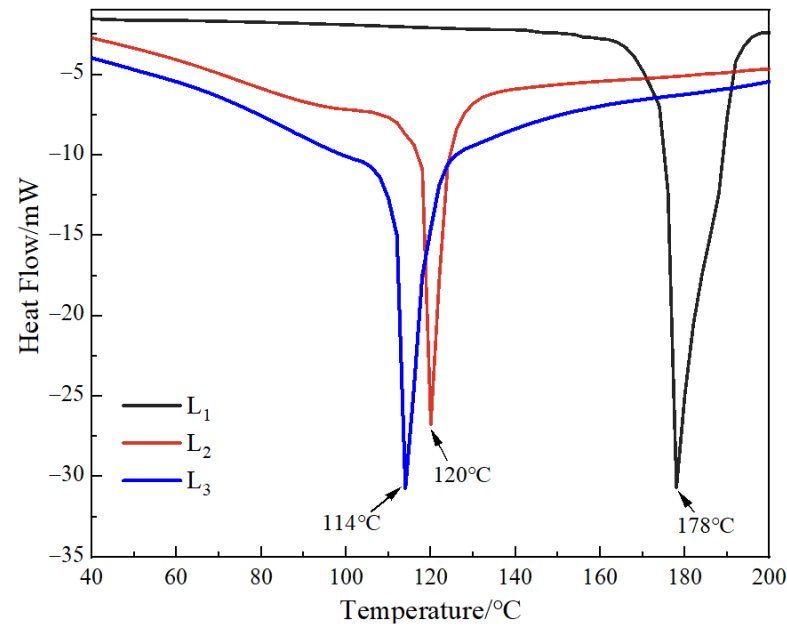


Figure 4. DSC thermograms of L₁, L₂, and L₃. L₁: the 2.5% SA one-layer-gel microspheres; L₂: the 2.5% SA two-layer-gel microspheres; L₃: the 2.5% SA three-layer-gel microspheres.

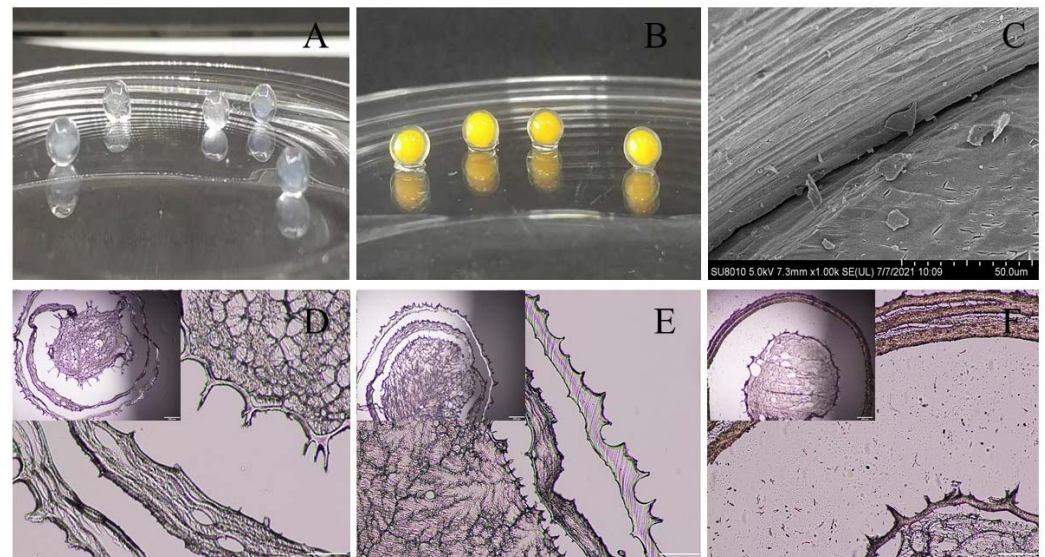


Figure 5. The digital photographs and microstructures of the gel microspheres. (A) Blank gel microspheres; (B) VB and BC-loaded-gel microspheres; (C) SEM photographs of cross sections of the microspheres; (D) Microscopic image of 0.5% SA three-layer-gel microspheres; (E) Microscopic image of 1.5% SA three-layer-gel microspheres; (F) Microscopic image of 2.5% SA three-layer-gel microspheres copy after sectioning the samples using a microtome.

3.6. Swelling Properties of the Gel Microspheres

The swelling behavior of the gel microspheres at pH 7.4, and 2.0 are shown in Figure 6. The percentage of swelling increased significantly ($p < 0.05$) with immersion time and the number of layers increased at pH 7.4. At approximately 4 h, the samples subjected to a pH of 7.4 were swollen to equilibrium and the swelling rate was more than 120% (Figure 6A). When the gel microspheres were placed in PBS, the swelling was mainly due to ion exchange between Ca^{2+} ions present in the “egg-box” cavity and Na^+ ions [22]. Because the Ca^{2+} ions present in poly guluronate blocks units are exchanged with Na^+ ions, and the carboxyl groups in SA electrostatically repel each other, thus the gel microspheres show swelling with the uptake of water [27,48].

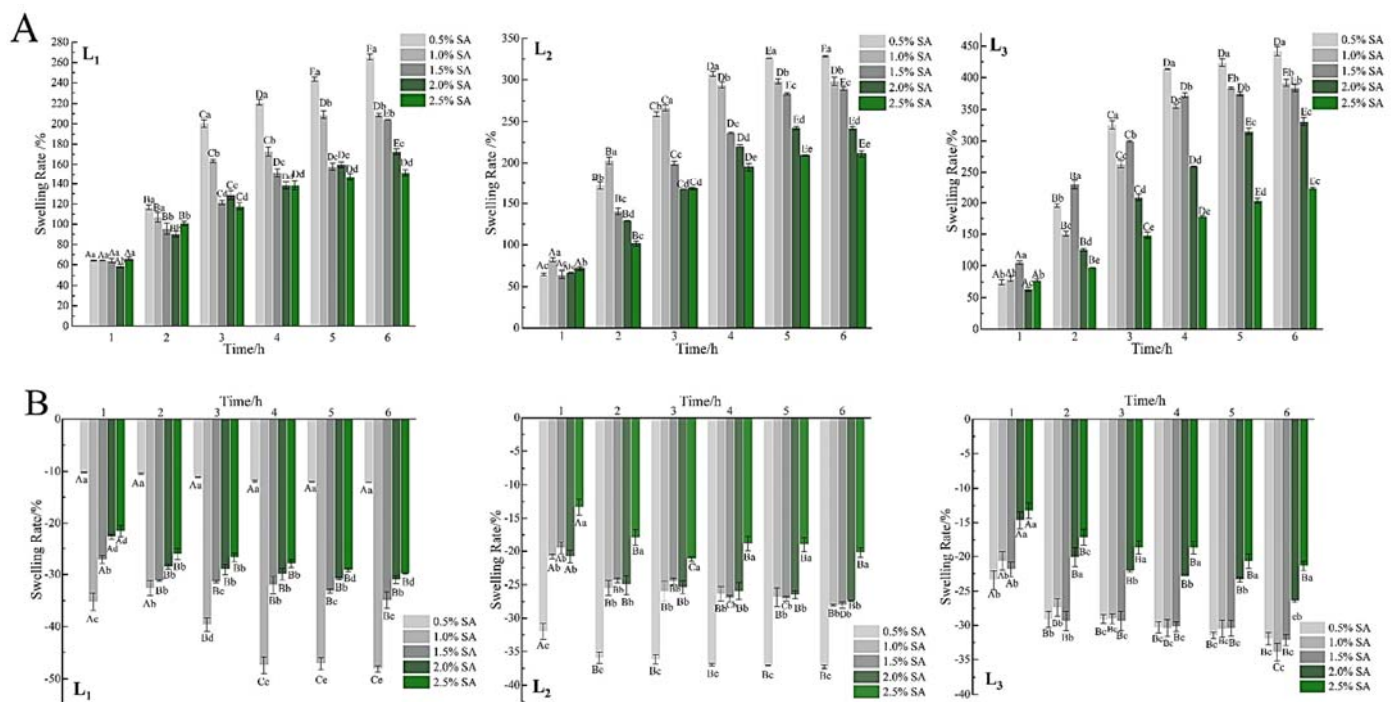


Figure 6. Swelling properties of the gel microspheres in phosphate-buffered solution with a pH of 7.4 (A) and 2.0 (B). L₁: the one-layer-gel microspheres; L₂: the two-layer-gel microspheres; L₃: the three-layer-gel microspheres. Different lowercase letters indicate significant differences ($p < 0.05$) of the swelling degree within the same time period. Different capital letters indicate significant differences ($p < 0.05$) of the swelling degree between different time periods at the same pH.

Interestingly, the mass of gel microspheres decreased, and the microspheres shrank slowly (Figure 6B). SA (pKa is 3.5 at 37 °C) gained a positive charge when the pH of the solution was 2.0, which would inhibit the cross-linking of carboxyl groups with calcium; then some Ca^{2+} ions were dissociated and released from the gel microspheres [43]. In addition, the gel microspheres maintained good sphericity throughout the test at a low pH. This supported that the existence of electrostatic interactions between protonated $-\text{NH}_3^+$ groups and unionized $-\text{COOH}$ groups under the acidic environments [49]. Thus, it may be concluded that the multilayered gel microspheres showed pH-responsive properties, which can remain stable in the harsh acidic environment of the stomach and protect the drugs from being destroyed.

3.7. In Vitro Release Studies of VB and BC from Gel Microspheres

According to the swelling characteristics, mechanical properties, and microstructure, the gel microspheres formed by 2.5% SA were submitted to study these conditions (e.g., single-layer-gel microspheres and multilayered gel microspheres), which could influence

the loading capacity of the BC/VB-loaded gel microspheres as well as the release of VB and BC in different encapsulation layers in vitro digestion. Compared to the VB loading capacity of L₁-VB (2.34 ± 1.51 mg/g), the VB loading capacity of L₃-VB was reduced to 2.03 ± 0.89 mg/g. This was due to diffusion of VB into the gel medium during the incubation phase. In Figure 7A, nearly 70.0% of VB was released from the L₃-VB and L₁-VB after only 2 h. Then the release of VB tended to gradually stabilize after 6 h; then the rest of the drug was slowly released. The VB is unstable under alkaline conditions, thus the rapid release of VB in the stomach, once it moves to the alkaline conditions of colon, which can quickly be absorbed. Release was divided into two main methods: drug release via degradation of the alginate network and drug diffusion through the alginate network for the drug release mechanism of the gel microspheres system [50]. When the gel microspheres were placed at pH 2.0, the COO⁻ groups of SA started to protonate, forming uncharged -COOH groups; thus, the alginate network became loose due to reduction in the degree of crosslinking of SA with Ca²⁺, and the electrostatic repulsion between the SA and CS increased [49]. Being water-soluble, VB quickly diffused into the solution through these loose network structures, leading to the burst release of VB. However, these release behaviors indicated that multilayer gel microspheres significantly retarded the release of VB as the number of layers increased. This phenomenon may be due to the network structure of the alginate gel; this structure may have limited the release of the drug [51].

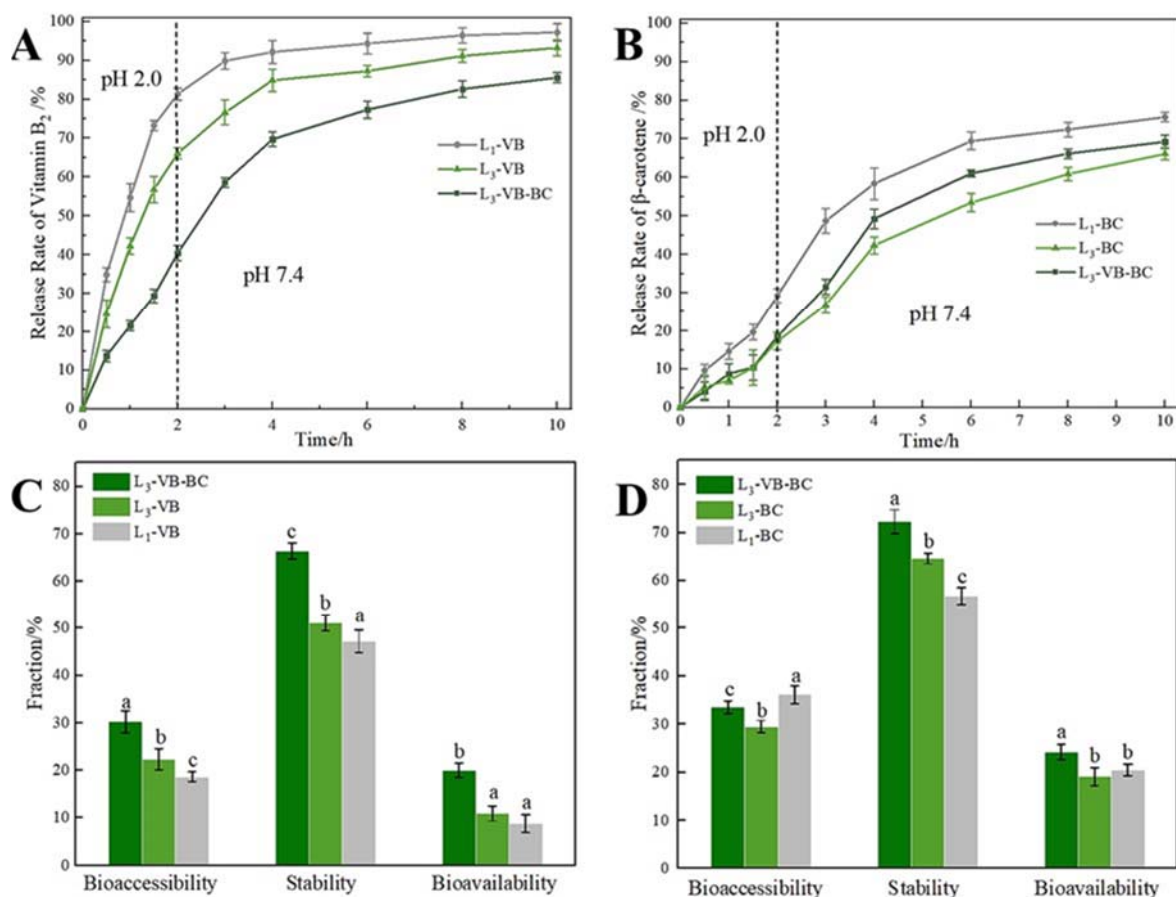


Figure 7. In vitro release studies of VB and BC from the gel microspheres. (A) The release profiles of VB from the gel microspheres; (B) The release profiles of BC from the gel microspheres; (C) Bioaccessibility, stability, and bioavailability of VB; (D) Bioaccessibility, stability, and bioavailability of BC. Different lowercase letters indicate significant differences ($p < 0.05$) of the same label.

There was no notable difference for the BC loading capacity of L₁-BC (2.92 ± 1.13 mg/g) and L₃-BC (2.88 ± 0.72 mg/g). Interestingly, the release behavior of BC was different from

that for VB. BC-loaded gel microspheres (Figure 7B) showed a sustained slow-release mode at pH 2.0, with less than 20% of BC being released within 2 h. This was due to the role of the outermost SA layer, which served as a diffusion barrier [22]. When BC-loaded gel microspheres were transferred into the artificial intestinal fluid (pH 7.4), they rapidly released the drug for nearly 4 h. When acidic/treated gel microspheres were transferred to the alkaline environment, the gel microspheres swelled faster but did not show higher water absorption values, which was related to loosening of their binding structures [52]. The protein was filled in a gel network that can help the gel microspheres absorb water faster [53]. Finally, the gel microspheres began to disintegrate along with the rapid release of BC.

For L₃-VB-BC, the VB and BC loading capacity were 2.79 ± 1.25 and 2.73 ± 1.10 mg/g, respectively. The enhanced VB loading capacity was related to the fact that the outer emulsion-filled gel layer can reduce the loss of VB. Moreover, the amount of VB released from L₃-VB-BC was lower than that from L₃-VB. The release of BC from gel microspheres was limited because of the hydrophobic of BC and its contact with the gel layer [18]. However, the release of BC from L₃-VB-BC was higher than that from L₃-BC, indicating that the dissolution of VB promoted the release of BC. An increase and decrease in the cumulative release of BC (69.24%) and VB (85.58%) were observed. This suggested that multilayered gel microspheres demonstrate the efficient delivery of bioactive substances in the colon, enabling the enhanced release of VB and BC in the intestinal tract.

Bioavailability and bioaccessibility can be used to evaluate the delivery efficiency of delivery systems [54]. In Figure 7C, the bioaccessibility and stability of VB are low for L₁-VB. There are two main reasons for that: firstly, VB readily dissolves in alkaline solutions [13]; and secondly, the VB dissolves quickly through these loose gel network structures. The bioavailability and stability of VB increased notably with the increase in the number of layers; this was related to the increase in the time required for its diffusion into the medium. The bioaccessibility of BC decreased with the numbers of layers, however, its stability increased significantly (Figure 7D). This was attributed to the gel layer and the presence of oil, which limited the release of BC. In addition, a certain amount of the BC was still encapsulated in the undigested lipid droplets [34]. For L₃-VB-BC, the bioaccessibility, stability and bioavailability of VB and BC were significantly improved (Figure 7C,D). This result indicated that the release of VB can improve the bioaccessibility of BC, and the release of BC also can improve the stability of VB. It also predicted that released BC was possibly limited by SA, CS and the formation of an emulsion in the solution medium; this may have contributed towards an increase in the stability of VB.

In general, the sustained release of VB or BC from multilayered gel microspheres was excellent; however, the low bioaccessibility and bioavailability of the encapsulated substances limited their delivery drugs into the gastrointestinal tract. The simultaneous encapsulation of VB and BC within multilayered gel microspheres notably improved their bioaccessibility and bioavailability. Considering that food needs to pass through the oral region to the gastric fluid and finally reach the intestine for digestion or absorption, the multilayer gel microspheres have the potential to simultaneously encapsulate and deliver multiple bioactive substances to the small intestine in these variable environments.

4. Conclusions

The results of FT-IR and XRD analysis confirmed the electrostatic interaction between CS and SA, and the VB and BC were encapsulated within the gel microspheres. The mechanical properties and particle size of these multilayered gel microspheres were controlled by the number of layers and the concentration of SA. The prepared multilayered gel microspheres were spherical and their clear core-shell structure was seen in the microscopic images. The swelling results exhibited remarkably diverse responses of multilayered gel microspheres to external conditions (pH 7.4, and 2.0). The multilayered gel microspheres showed more delay in the release of VB and BC, compared with the one-layer VB-loaded gel microspheres or one-layer BC-loaded gel. The release behavior of VB and BC-loaded

gel microspheres suggested that released BC was possibly restricted by SA, CS and the formation of the emulsion, which improved stability of VB. The simultaneous encapsulation of VB and BC within multilayered gel microspheres notably improved their bioaccessibility and bioavailability. The above results indicated that the multilayered gel microspheres had the ability to simultaneously encapsulate water-soluble and lipid-soluble bioactive substances, enabling the delivery of these substances into the gastrointestinal tract. Thus, the multilayered gel microspheres show great potential as delivery systems for improving the digestion and absorption of multilayer-gel-encapsulated nutrients in the body.

Author Contributions: Investigation and writing—original draft, P.L.; conceptualization and software, S.D. and Z.L.; supervision, X.T.; validation and formal analysis, S.Y. and Y.C.; resources and data curation, W.Q. and X.P.; supervision and writing—review and editing, H.W. and L.J. All authors have read and agreed to the published version of the manuscript.

Funding: This research was funded by the Excellent Youth Project of Natural Science Foundation of Heilongjiang Province, Grant No. YQ2021C023; Funding for the Opening Project of Key Laboratory of Soybean Biology of Chinese Education Ministry, Grant NO. SBKF13, and the “Young Talents” Project of Northeast Agricultural University, Grant No. 19QC29.

Conflicts of Interest: The authors declare no conflict of interest.

References

1. Benucci, I.; Lombardelli, C.; Cacciotti, I.; Liburdi, K.; Nanni, F.; Esti, M. Chitosan beads from microbial and animal sources as enzyme supports for wine application. *Food Hydrocoll.* **2016**, *61*, 191–200. [[CrossRef](#)]
2. Chandrasekar, V.; Coupland, J.N.; Anantheswaran, R.C. Characterization of nisin containing chitosan-alginate microparticles. *Food Hydrocoll.* **2017**, *69*, 301–307. [[CrossRef](#)]
3. Loyeau, P.A.; Spotti, M.J.; Vinderola, G.; Carrara, C.R. Encapsulation of potential probiotic and canola oil through emulsification and ionotropic gelation, using protein/polysaccharides Maillard conjugates as emulsifiers. *LWT* **2021**, *150*, 111980. [[CrossRef](#)]
4. Ma, D.; Tu, Z.-C.; Wang, H.; Zhang, Z.; McClements, D.J. Fabrication and characterization of nanoemulsion-coated microgels: Electrostatic deposition of lipid droplets on alginate beads. *Food Hydrocoll.* **2017**, *71*, 149–157. [[CrossRef](#)]
5. Hu, S.-H.; Chen, S.-Y.; Gao, X. Multifunctional Nanocapsules for Simultaneous Encapsulation of Hydrophilic and Hydrophobic Compounds and On-Demand Release. *ACS Nano* **2012**, *6*, 2558–2565. [[CrossRef](#)] [[PubMed](#)]
6. Kalaycioglu, G.D.; Aydogan, N. Layer-by-layer coated microcapsules with lipid nanodomains for dual-drug delivery. *Colloids Surf. A Physicochem. Eng. Asp.* **2020**, *584*, 124037. [[CrossRef](#)]
7. Grigoriev, D.O.; Bukreeva, T.; Möhwald, H.; Shchukin, D. New Method for Fabrication of Loaded Micro- and Nanocontainers: Emulsion Encapsulation by Polyelectrolyte Layer-by-Layer Deposition on the Liquid Core. *Langmuir* **2008**, *24*, 999–1004. [[CrossRef](#)]
8. Somo, S.I.; Khanna, O.; Brey, E.M. Alginate Microbeads for Cell and Protein Delivery. In *Advanced Structural Safety Studies*; Springer: Singapore, 2017; Volume 1479, pp. 217–224.
9. Liu, K.; Chen, Y.-Y.; Zha, X.-Q.; Li, Q.-M.; Pan, L.-H.; Luo, J.-P. Research progress on polysaccharide/protein hydrogels: Preparation method, functional property and application as delivery systems for bioactive ingredients. *Food Res. Int.* **2021**, *147*, 110542. [[CrossRef](#)]
10. Su, C.-W.; Chiang, C.-S.; Li, W.-M.; Hu, S.-H.; Chen, S.-Y. Multifunctional nanocarriers for simultaneous encapsulation of hydrophobic and hydrophilic drugs in cancer treatment. *Nanomedicine* **2014**, *9*, 1499–1515. [[CrossRef](#)]
11. Hu, Q.; Sun, W.; Wang, C.; Gu, Z. Recent advances of cocktail chemotherapy by combination drug delivery systems. *Adv. Drug Deliv. Rev.* **2016**, *98*, 19–34. [[CrossRef](#)] [[PubMed](#)]
12. Araki, A.; Yoshimura, Y.; Sakurai, T.; Umegaki, H.; Kamada, C.; Iimuro, S.; Ohashi, Y.; Ito, H.; The Japanese Elderly Diabetes Intervention Trial Research Group. Low intakes of carotene, vitamin B2, pantothenate and calcium predict cognitive decline among elderly patients with diabetes mellitus: The Japanese Elderly Diabetes Intervention Trial. *Geriatr. Gerontol. Int.* **2017**, *17*, 1168–1175. [[CrossRef](#)] [[PubMed](#)]
13. Halver, J.E. The Vitamins. In *Fish Nutrition*; Elsevier BV: Amsterdam, The Netherlands, 2003; pp. 61–141.
14. Valentine, M.E.; Kirby, B.D.; Withers, T.R.; Johnson, S.L.; Long, T.E.; Hao, Y.; Lam, J.S.; Niles, R.M.; Yu, H.D. Generation of a highly attenuated strain of *Pseudomonas aeruginosa* for commercial production of alginate. *Microb. Biotechnol.* **2019**, *13*, 162–175. [[CrossRef](#)]
15. George, M.; Abraham, T.E. Polyionic hydrocolloids for the intestinal delivery of protein drugs: Alginate and chitosan—A review. *J. Control. Release* **2006**, *114*, 1–14. [[CrossRef](#)] [[PubMed](#)]
16. Zou, L.; Zhang, Z.; Zhang, R.; Liu, W.; Liu, C.; Xiao, H.; McClements, D.J. Encapsulation of protein nanoparticles within alginate microparticles: Impact of pH and ionic strength on functional performance. *J. Food Eng.* **2016**, *178*, 81–89. [[CrossRef](#)]

17. Bajpai, S.; Tankhiwale, R. Investigation of dynamic release of vitamin B2 from calcium alginate/chitosan multilayered beads: Part II. *React. Funct. Polym.* **2006**, *66*, 1565–1574. [[CrossRef](#)]
18. Feng, W.; Yue, C.; Wusigale, Ni, Y.; Liang, L. Preparation and characterization of emulsion-filled gel beads for the encapsulation and protection of resveratrol and α -tocopherol. *Food Res. Int.* **2018**, *108*, 161–171. [[CrossRef](#)] [[PubMed](#)]
19. Silva, K.C.G.; Feltre, G.; Hubinger, M.D.; Sato, A.C.K. Protection and targeted delivery of β -carotene by starch-alginate-gelatin emulsion-filled hydrogels. *J. Food Eng.* **2021**, *290*, 110205. [[CrossRef](#)]
20. Qin, C.; Zhou, J.; Zhang, Z.; Chen, W.; Hu, Q.; Wang, Y. Convenient one-step approach based on stimuli-responsive sol-gel transition properties to directly build chitosan-alginate core-shell beads. *Food Hydrocoll.* **2019**, *87*, 253–259. [[CrossRef](#)]
21. Birch, N.P.; Barney, L.E.; Pandres, E.; Peyton, S.R.; Schiffman, J.D. Thermal-Responsive Behavior of a Cell Compatible Chitosan/Pectin Hydrogel. *Biomacromolecules* **2015**, *16*, 1837–1843. [[CrossRef](#)]
22. Bajpai, S.; Tankhiwale, R. Investigation of water uptake behavior and stability of calcium alginate/chitosan bi-polymeric beads: Part-1. *React. Funct. Polym.* **2006**, *66*, 645–658. [[CrossRef](#)]
23. Pasparakis, G.; Bouropoulos, N. Swelling studies and in vitro release of verapamil from calcium alginate and calcium alginate-chitosan beads. *Int. J. Pharm.* **2006**, *323*, 34–42. [[CrossRef](#)] [[PubMed](#)]
24. Ji, M.; Sun, X.; Guo, X.; Zhu, W.; Wu, J.; Chen, L.; Wang, J.; Cheng, C.; Zhang, Q. Green synthesis, characterization and in vitro release of cinnamaldehyde/sodium alginate/chitosan nanoparticles. *Food Hydrocoll.* **2019**, *90*, 515–522. [[CrossRef](#)]
25. Belščak-Cvitanović, A.; Bušić, A.; Barišić, L.; Vrsaljko, D.; Karlović, S.; Špoljarić, I.; Vojvodić, A.; Mršić, G.; Komes, D. Emulsion templated microencapsulation of dandelion (*Taraxacum officinale* L.) polyphenols and β -carotene by ionotropic gelation of alginate and pectin. *Food Hydrocoll.* **2016**, *57*, 139–152. [[CrossRef](#)]
26. Yadav, S.K.; Khan, G.; Bonde, G.; Bansal, M.; Mishra, B. Design, optimization and characterizations of chitosan fortified calcium alginate microspheres for the controlled delivery of dual drugs. *Artif. Cells Nanomed. Biotechnol.* **2017**, *46*, 1180–1193. [[CrossRef](#)]
27. Sun, X.; Liu, C.; Omer, A.; Yang, L.-Y.; Ouyang, X.-K. Dual-layered pH-sensitive alginate/chitosan/kappa-carrageenan microbeads for colon-targeted release of 5-fluorouracil. *Int. J. Biol. Macromol.* **2019**, *132*, 487–494. [[CrossRef](#)] [[PubMed](#)]
28. Ma, D.; Tu, Z.-C.; Wang, H.; Zhang, Z.; McClements, D.J. Microgel-in-Microgel Biopolymer Delivery Systems: Controlled Digestion of Encapsulated Lipid Droplets under Simulated Gastrointestinal Conditions. *J. Agric. Food Chem.* **2018**, *66*, 3930–3938. [[CrossRef](#)]
29. Fareez, I.M.; Lim, S.M.; Mishra, R.K.; Ramasamy, K. Chitosan coated alginate-xanthan gum bead enhanced pH and thermotolerance of *Lactobacillus plantarum* LAB12. *Int. J. Biol. Macromol.* **2015**, *72*, 1419–1428. [[CrossRef](#)] [[PubMed](#)]
30. Lin, D.; Kelly, A.L.; Maidannyk, V.; Miao, S. Effect of concentrations of alginate, soy protein isolate and sunflower oil on water loss, shrinkage, elastic and structural properties of alginate-based emulsion gel beads during gelation. *Food Hydrocoll.* **2020**, *108*, 105998. [[CrossRef](#)]
31. Donhowe, E.G.; Flores, F.P.; Kerr, W.L.; Wicker, L.; Kong, F. Characterization and in vitro bioavailability of β -carotene: Effects of microencapsulation method and food matrix. *LWT* **2014**, *57*, 42–48. [[CrossRef](#)]
32. Roman, M.J.; Burri, B.J.; Singh, R.P. Release and Bioaccessibility of β -Carotene from Fortified Almond Butter during in Vitro Digestion. *J. Agric. Food Chem.* **2012**, *60*, 9659–9666. [[CrossRef](#)] [[PubMed](#)]
33. Umaredkar, A.A.; Dangre, P.V.; Mahapatra, D.K.; Dhabarde, D.M. Fabrication of chitosan-alginate polyelectrolyte complexed hydrogel for controlled release of cilnidipine: A statistical design approach. *Mater. Technol.* **2020**, *35*, 697–707. [[CrossRef](#)]
34. Han, J.; Zhang, Z.; Shang, W.; Yan, J.; McClements, D.; Xiao, H.; Wu, H.; Zhu, B. Modulation of physicochemical stability and bioaccessibility of β -carotene using alginate beads and emulsion stabilized by scallop (*Patinopecten yessoensis*) gonad protein isolates. *Food Res. Int.* **2020**, *129*, 108875. [[CrossRef](#)] [[PubMed](#)]
35. Türkoğlu, G.C.; Saruşık, A.M.; Karavana, S.Y. Development of textile-based sodium alginate and chitosan hydrogel dressings. *Int. J. Polym. Mater.* **2020**, *70*, 916–925. [[CrossRef](#)]
36. Yousefi, M.; Khanniri, E.; Shadnoush, M.; Khorshidian, N.; Mortazavian, A.M. Development, characterization and in vitro antioxidant activity of chitosan-coated alginate microcapsules entrapping *Viola odorata* Linn. extract. *Int. J. Biol. Macromol.* **2020**, *163*, 44–54. [[CrossRef](#)] [[PubMed](#)]
37. Liu, H.; Liu, F.; Ma, Y.; Goff, H.D.; Zhong, F. Versatile preparation of spherically and mechanically controllable liquid-core-shell alginate-based bead through interfacial gelation. *Carbohydr. Polym.* **2020**, *236*, 115980. [[CrossRef](#)]
38. Letona, C.A.M.; Park, C.-S.; Kim, Y.-R. Amylosucrase-mediated β -carotene encapsulation in amylose microparticles. *Biotechnol. Prog.* **2017**, *33*, 1640–1646. [[CrossRef](#)]
39. Vaziri, A.S.; Alemzadeh, I.; Vossoughi, M. Improving survivability of *Lactobacillus plantarum* in alginate-chitosan beads reinforced by Na-tripolyphosphate dual cross-linking. *LWT* **2018**, *97*, 440–447. [[CrossRef](#)]
40. Bonda, A.F.; Regis, L.; Giovannelli, L.; Segale, L. Alginate/maltodextrin and alginate/shellac gum core-shell capsules for the encapsulation of peppermint essential oil. *Int. J. Biol. Macromol.* **2020**, *162*, 1293–1302. [[CrossRef](#)] [[PubMed](#)]
41. Rahiminezhad, Z.; Gahruie, H.H.; Esteghlal, S.; Mesbahi, G.R.; Golmakani, M.-T.; Hosseini, S.M.H. Oxidative stability of linseed oil nano-emulsions filled in calcium alginate hydrogels. *LWT* **2020**, *127*, 109392. [[CrossRef](#)]
42. Anal, A.K.; Bhopatkar, D.; Tokura, S.; Tamura, H.; Stevens, W.F. Chitosan-Alginate Multilayer Beads for Gastric Passage and Controlled Intestinal Release of Protein. *Drug Dev. Ind. Pharm.* **2003**, *29*, 713–724. [[CrossRef](#)]
43. Li, Y.; Kong, M.; Feng, C.; Liu, W.F.; Liu, Y.; Cheng, X.J.; Chen, X.G. Preparation and property of layer-by-layer alginate hydrogel beads based on multi-phase emulsion technique. *J. Sol-Gel Sci. Technol.* **2012**, *62*, 217–226. [[CrossRef](#)]

44. Miura, K.; Kimura, N.; Suzuki, H.; Miyashita, Y.; Nishio, Y. Thermal and viscoelastic properties of alginate/poly(vinyl alcohol) blends cross-linked with calcium tetraborate. *Carbohydr. Polym.* **1999**, *39*, 139–144. [[CrossRef](#)]
45. Li, X.; Xie, H.; Lin, J.; Xie, W.; Ma, X. Characterization and biodegradation of chitosan–alginate polyelectrolyte complexes. *Polym. Degrad. Stab.* **2009**, *94*, 1–6. [[CrossRef](#)]
46. Honary, S.; Maleki, M.; Karami, M. The effect of chitosan molecular weight on the properties of alginate/ chitosan microparticles containing prednisolone. *Trop. J. Pharm. Res.* **2009**, *8*, 53–61. [[CrossRef](#)]
47. Lim, G.-P.; Lee, B.-B.; Ahmad, M.S.; Singh, H.; Ravindra, P. Influence of process variables and formulation composition on sphericity and diameter of Ca-alginate-chitosan liquid core capsule prepared by extrusion dripping method. *Part. Sci. Technol.* **2016**, *34*, 681–690. [[CrossRef](#)]
48. van Leusden, P.; Hartog, G.D.; Bast, A.; Postema, M.; van der Linden, E.; Sagis, L. Permeation of probe molecules into alginate microbeads: Effect of salt and processing. *Food Hydrocoll.* **2017**, *73*, 255–261. [[CrossRef](#)]
49. Li, J.; Jiang, C.; Lang, X.; Kong, M.; Cheng, X.; Liu, Y.; Feng, C.; Chen, X. Multilayer sodium alginate beads with porous core containing chitosan based nanoparticles for oral delivery of anticancer drug. *Int. J. Biol. Macromol.* **2016**, *85*, 1–8. [[CrossRef](#)]
50. Dragana, M.; Aleksandra, Z.; Nikola, S.; Marija, V.; Milorad, C.; Goran, N. Alginates and similar exopolysaccharides in biomedical application and pharmacy: Controlled delivery of drugs. *Adv. Technol.* **2016**, *5*, 39–52. [[CrossRef](#)]
51. Zhao, Q.S.; Ji, Q.X.; Cheng, X.J.; Sun, G.Z.; Ran, C.; Zhao, B.; Chen, X.G. Preparation of alginate coated chitosan hydrogel beads by thermosensitive internal gelation technique. *J. Sol-Gel Sci. Technol.* **2010**, *54*, 232–237. [[CrossRef](#)]
52. Bajpai, S.; Sharma, S. Investigation of swelling/ degradation behaviour of alginate beads crosslinked with Ca²⁺ and Ba²⁺ ions. *React. Funct. Polym.* **2004**, *59*, 129–140. [[CrossRef](#)]
53. Volić, M.; Pajić-Lijaković, I.; Djordjević, V.; Knežević-Jugović, Z.; Pećinar, I.; Stevanović-Dajić, Z.; Veljovic, D.; Hadnadjev, M.; Bugarski, B. Alginate/soy protein system for essential oil encapsulation with intestinal delivery. *Carbohydr. Polym.* **2018**, *200*, 15–24. [[CrossRef](#)] [[PubMed](#)]
54. Jain, S.; Winuprasith, T.; Suphantharika, M. Encapsulation of lycopene in emulsions and hydrogel beads using dual modified rice starch: Characterization, stability analysis and release behaviour during in-vitro digestion. *Food Hydrocoll.* **2020**, *104*, 105730. [[CrossRef](#)]